

## Histosol pedogenesis in floodplain coastal environments in the state of Rio de Janeiro, Brazil

Paula Fernanda Chaves Soares<sup>a</sup>, Rafael Cipriano da Silva<sup>b</sup>, Eduardo Carvalho da Silva Neto<sup>c</sup>, Marcos Gervasio Pereira<sup>c,\*</sup>, Carlos Roberto Pinheiro Junior<sup>c</sup>, Luiz Carlos Ruiz Pessenda<sup>d</sup>, Lúcia Helena Cunha dos Anjos<sup>c</sup>

<sup>a</sup> Universidade Iguaçú, Nova Iguaçú, Av. Afílio Augusto Távora, 2134, Rio de Janeiro, Brazil

<sup>b</sup> Fundação Cearense de Meteorologia, Av. Rui Barbosa, 1246, Fortaleza, Ceará, Brazil

<sup>c</sup> Universidade Federal Rural do Rio de Janeiro, Instituto de Agronomia, Departamento de Solos, BR-465, Seropédica, Rio de Janeiro, Brazil

<sup>d</sup> Universidade de São Paulo, Centro de Energia Nuclear na Agricultura, Piracicaba, São Paulo, Brazil

### ARTICLE INFO

#### Keywords:

Histic horizon  
Organic matter  
Carbon and nitrogen isotopes  
Dating

### ABSTRACT

This study aimed to evaluate the morphological, physical, and chemical properties of Histosols in wetlands and to infer aspects related to their pedogenesis based on C and N isotopes and <sup>14</sup>C dating to better understand ecosystem services, paleo-environments, and post-depositional processes based on preliminary results. Two Histosol pedons, located in different floodplains that refer to different sedimentation environments, were sampled in the state of Rio de Janeiro. Morphological, physical, and chemical characterization were performed, and the total C and N content of the substrate and the C content of humic substances were assessed. Elemental C and N and isotope analyses ( $\delta^{13}\text{C}$  and  $\delta^{15}\text{N}$ ) were performed every 10 cm, while <sup>14</sup>C dating of the humin fraction was performed at 40–50 and 190–200 cm. The interproxy approach combining pedological analyses, radiocarbon dating, and elemental and isotopic analyses of total C and N of organic matter, showed a mixture of algae and continental/terrestrial organic matter deposited in peatlands, over the last ~ 4000 cal years before present (BP). The studied soils were formed by geogenic and pedogenic processes (terrestrialization, paludization, and aggradation). Considering the relationships between  $\delta^{13}\text{C}$  and  $\delta^{15}\text{N}$ , between C/N and  $\delta^{13}\text{C}$ , and the soil characteristics, these deposits were probably formed by vertical accretion in lake environments. However, near 2300 cal yr BP, the radiocarbon dating and isotopic analyses suggest the occurrence of deposition of alluvial sediments transported by the Suruí River in RJ-01. It is likely that the modern age obtained by <sup>14</sup>C dating in RJ-02, near 3600 cal yr BP, is probably due to the intense bioturbation by plant roots and the input of young material during the seasonal flood period.

### 1. Introduction

Wetlands are global hotspots of biological diversity and consist of complex ecosystems that are important for economic activities, especially agriculture (Valladares et al., 2007; Campos et al., 2010; Gumbrecht et al., 2017). Peatlands are a subset of environments within wetlands and are formed from the accumulation of significant amounts of organic matter in the soil. The irreversible alteration and humification of this organic matter is related to the pedogenetic process of paludization, and its accumulation in layers greater than 40 cm characterizes soils classified as Histosols (Buol et al., 2011). Histosols contain records that allow the reconstruction of environments in the Late Quaternary,

including time of formation, vegetation, and climatic variations. The parent material of these soils is strongly associated with vegetation, which influences their formation. The type and amount of organic material that accumulates depends on the source of the organic matter and its rates of deposition and decomposition, factors that influence the availability of oxygen, and climatic conditions, which are defined by the climate and the relief (Lamb et al., 2006; Silva Neto et al., 2019).

Coastal environments commonly preserve thick sequences of Holocene sediments, offering the opportunity to investigate past climates as well as more local environmental changes. Previous studies report that the  $\delta^{13}\text{C}$ ,  $\delta^{15}\text{N}$ , and C/N values of the sedimentary organic matter depend on the environment (Lamb et al., 2006; Buso Junior et al., 2013;

\* Corresponding author.

E-mail address: [gervasio@ufrj.br](mailto:gervasio@ufrj.br) (M.G. Pereira).

Silva Neto et al., 2019). According to Lamb et al. (2006), the  $C_3$  terrestrial plants have  $\delta^{13}C$  values and C/N ratios between  $-32\text{‰}$  and  $-21\text{‰}$  and  $>12$ , respectively. Freshwater and marine algae have  $\delta^{13}C$  values between  $-30\text{‰}$  and  $-25\text{‰}$ , and  $-24\text{‰}$  to  $-18\text{‰}$ , respectively. Algae have C/N ratios between 10 and 6. Sedimentary organic matter from terrestrial and aquatic plants exhibit  $\delta^{15}N$  values of  $\sim 0\text{‰}$  and  $10\text{‰}$ , respectively (Deines, 1980; Meyers, 1994).

The comparison of properties in Histosols, as the characterization of organic matter and humic substances, has provided a reliable paleoenvironmental proxy. In addition, this evaluation is important because it helps in understanding the studies related to different age and/or occupation conditions in different regions. Considering their multiple ecosystem services, the need for the conservation of wetlands and, therefore, Histosols is widely acknowledged but long challenged by national development policies and economic priorities. Thus, drainage, fires, and conversion to agriculture are currently transforming peatlands and soils present in these environments (Santos et al., 2020).

South America accounts for approximately 46% of all tropical peatland areas of wetlands, which are estimated to cover an area of  $312,250 \text{ km}^2$  in Brazil (Gumbrecht et al., 2017). Histosols occur in wetlands in coastal plains, deltas, and inland river and lake areas, with limited drainage promoting organic matter (OM) accumulation (Soil Survey Staff, 2010; Junk et al., 2013; Bispo et al., 2015; Santos et al., 2018).

The state of Rio de Janeiro has a coastline of 1160 km, with a high population density, which directly or indirectly depends on ecosystem services provided by coastal ecosystems, including the peat environments of wetlands. The hydrographic region of Guanabara Bay is a model of a coastal system occurrence of peatland, which suffers from the strong impact of anthropic action and with a rapid process of

degradation and eutrophication of water bodies due to the release of sewage, which is produced by approximately 12 million inhabitants (Costa et al., 2018). In the northern region of the state, which is also characterized by vast wetlands, the process of occupation and agricultural use of peatland areas was intensified through flood control programs conducted in the 1940s, when large drainage systems were built (Lima et al., 2013).

The general hypothesis of this study is based on the premise that the intrinsic parameters of Histosols are related to pedogenetic factors and paleoenvironmental studies. Thus, the objective of this study was to evaluate the morphological, chemical and physical characteristics of Histosols in a floodplain, to infer aspects related to pedogenesis, and to characterize the soil organic matter origin based on C and N isotope analysis and  $^{14}C$  dating. The main objectives of this study were to identify the presence of peatlands in floodplain coastal environments in the state of Rio de Janeiro, Brazil, and to characterize the soils of these environments. For this, a detailed study of two soil cores was carried out, including analysis of morphological characteristics, chemical and physical properties, elemental composition (CHN), and variation of carbon ( $^{13}C$  and  $^{14}C$ ) and nitrogen ( $^{15}N$ ) isotopes. These isotope studies are a preliminary evaluation in this area, and the information obtained can guide the sustainable management and prevention of soil degradation in these areas or its preservation in natural conditions to avoid environmental impacts in the adjacent areas.

## 2. Material and methods

### 2.1. Regional settings

The study area comprises two areas of peatlands in floodplain coastal

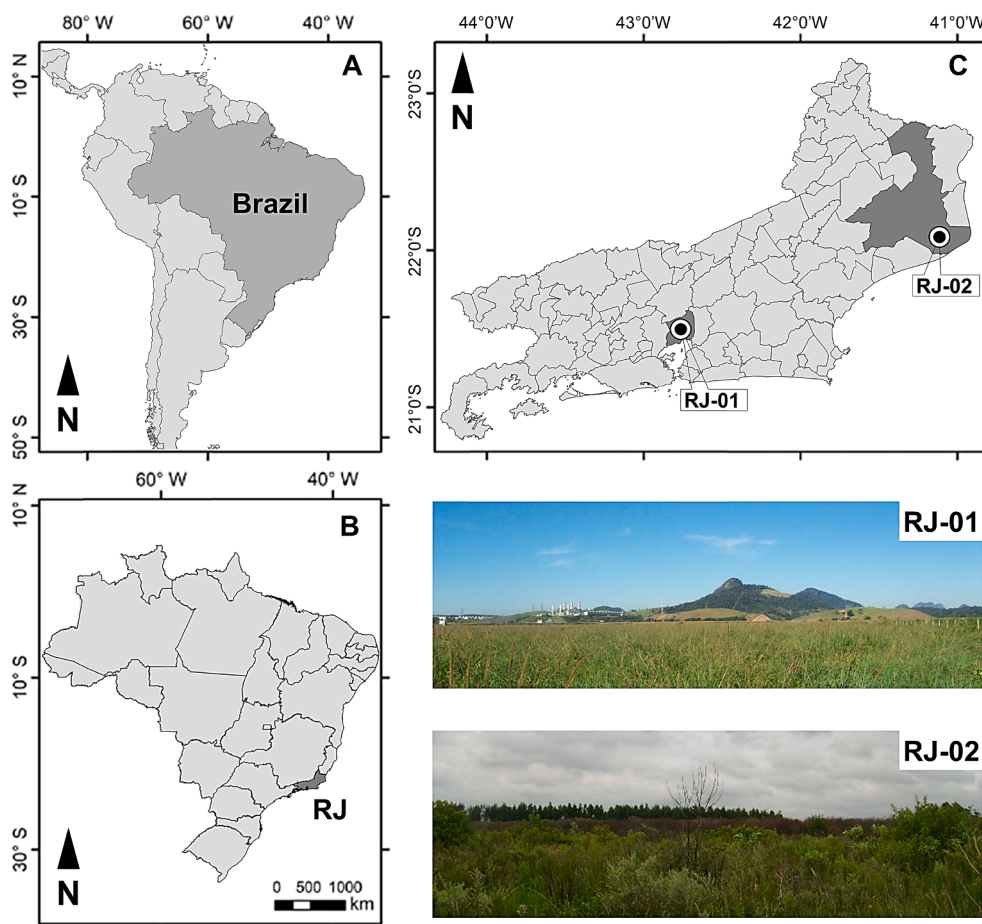


Fig. 1. Study areas locations in floodplain environments in Rio de Janeiro State, Brazil.

environments in the state of Rio de Janeiro, Brazil (Fig. 1, Table 1), both located in the same topographic position, with an altitude of approximately 3 m. The areas were selected from soil surveys and previous pedological studies, in addition to being representative environments of peat soils that occur in the state of Rio de Janeiro. In addition, these areas were selected because they refer to different sedimentation environments along the coastline of this state (Luz et al., 2011; Lima et al., 2013; Costa et al., 2018).

Pedon 1 (RJ-01) was described and sampled in the municipality of Magé. The area is included in the hydrographic region of Guanabara Bay, spanning approximately 4,066 km<sup>2</sup> (Costa et al., 2018), and the soil is located near the Suruí River. In the central strip of the municipality, there is a dissected relief of pre-Cambrian geology (Suruí granite) (Lemos, 2002). The soil core collection area is part of the Holocene fluvial-marine sediment (Magé Formation), where the formation of terraces and sandbanks occurred after the Ganabarian Transgression (Amador, 1997). Lithologically, they are made up of fine, silty-clayey, or clay-silty sediments that are rich in organic matter (Amador, 1997). Pedon 2 (RJ-02), located in the municipality of Campos dos Goytacazes, was sampled in the region of the Lagoa Feia sub-basin. The region is known as *Baixada Campista* and encompasses an area of floodplain and restingas marked by seasonal floods between the dry and rainy seasons (Luz et al., 2011; Lima et al., 2013). The source material consists of deposits of fluvial-marine sediments accumulated during the Holocene, when the mouth of the Paraíba do Sul River shifted northward, abandoning an inland delta. Both areas (RJ-01 and RJ-02) had a high degree of environmental degradation, with a marked reduction in the original mangrove area. The relief is flat, with wide areas of coastal lowland in contrast to the relief to the north, dominated by the north by the escarpment of Serra do Mar, with mountainous relief (IBGE, 2008). The climate is type Aw, according to the Köppen climate classification, with an annual average temperature of 27 °C and annual average rainfall of 1500 mm for RJ-01, and with a 24 °C annual average temperature and 1100 mm annual average rainfall, unevenly distributed, with dry seasons with high temperatures for RJ-02 (Alvares et al., 2013). The vegetation of the area is characterized as a restinga forest, which is part of the Atlantic Forest biome.

## 2.2. Soil sampling

Two pedons were selected from the floodplain environments of the Rio de Janeiro State, Brazil (Fig. 2). The pedons were collected using a vibrocorer. The intact soil monoliths were transported to the laboratory of the Federal Rural University of Rio de Janeiro (UFRRJ), where the collection tube was opened to take samples at 10 cm intervals for C (<sup>14</sup>C and <sup>δ<sup>13</sup>C</sup>) and N (<sup>δ<sup>15</sup>N</sup>) isotope analyses. In addition, a trench was opened for soil sampling and description pedologically according to the soil horizons. The pedons were described morphologically (Fig. 2) and sampled according to Santos et al. (2015) for further classification according to Soil Taxonomy (Soil Survey Staff, 2014) and Brazilian Soil Classification System (*Sistema Brasileiro de Classificação do Solo* – SiBCS) (Santos et al., 2018).

**Table 1**  
Information about of the Histosols in floodplain environment of Rio de Janeiro State, Brazil.

Profile	Region	Landscape position	Water table (cm)	Coordinates
RJ-01	Magé	Floodplain, in de back of Guanabara Bay	40	22° 36' 54.24" S 43° 6' 41.95" W
RJ-02	Campos dos Goytacazes	Floodplain, margin of Lagoa Feia	50	21° 52' 22.62" S 41° 28' 35.94" W

## 2.3. Soil analyses

The physical and chemical properties were analyzed according to the characterization tests of Histosols (Lynn et al., 1974), as described by Santos et al. (2018). The rubbed fibers (RF), pyrophosphate index (PI), and the von Post scale (VP) were used to assess the degree of peat decomposition (Staneek and Silc, 1977). The values of pH in water (1:2.5 soil solution ratio), exchangeable bases (Ca<sup>+2</sup>, Mg<sup>+2</sup>, K<sup>+2</sup> and Na<sup>+</sup>), exchangeable Al<sup>+3</sup>, potential acidity (H + Al), and available P were determined for chemical characterization. The following parameters were calculated: sum of bases (S = Ca<sup>+2</sup> + Mg<sup>+2</sup> + K<sup>+</sup> + Na<sup>+</sup>), cation exchange capacity (CEC = S + H + Al), percentage of exchangeable sodium (Na% = Na × 100 / CEC), and saturation by exchangeable Al<sup>+3</sup> (m% = Al<sup>+3</sup> × 100 / CEC) (IUSS Working Group WRB, 2015; Teixeira et al., 2017).

Elemental concentrations were determined in dried, milled, and homogenized samples of 10 cm thickness. The C, H, and N contents of the soil cores were determined using an elemental analyzer (CHN analyzer, TrueSpec Series: Carbon, Hydrogen, Nitrogen, Macro) coupled to a mass spectrometer hosted in the *Laboratório de Isótopos Estáveis de the Centro de Energia Nuclear na Agricultura* — CENA/USP (Piracicaba, SP, Brazil). Elemental results were used to calculate the C:N ratios of the soil samples. The chemical fractionation of humic substances was performed according to the method recommended by the International Humic Substances Society, with the methodological protocol described by Swift (1996), assessing the C content of humin (C-HUM), humic acid (C-HA), and fulvic acid (C-FA) fractions and determining the C-FA/C-HA ratio.

The following physical characterization analyses were performed on the soil horizon samples: bulk density (Bd), particle (Pd) density, gravimetric moisture (Gh), and total pore volume (TPV) (Andriess, 1988; Teixeira et al., 2017). In addition, the organic matter (OM) content was quantified using the weight loss method by incineration at 500 °C in a muffle furnace. The values of organic matter density (OMD), minimum residue (MR), and mineral material (MM) were also determined according to Lynn et al. (1974) using the methodology described by (Santos et al., 2018).

Soil material was collected at 10 cm intervals until reaching a depth of 200 cm to analyze stable isotopes. The samples were dried in an oven at 45 °C for 24 h, pounded to break up the clods, macerated using a mortar and pestle, passed through a 100-mesh sieve, and sent to the Stable Isotopes Laboratory of the Center for Nuclear Energy in Agriculture (*Centro de Energia Nuclear na Agricultura* – CENA) to determine the <sup>δ<sup>13</sup>C</sup> and <sup>δ<sup>15</sup>N</sup> values. These analyses were performed on a Finnigan Delta Plus mass spectrophotometer coupled to a C and total N auto-analyzer, Carlo Erba AE1108 - Finnigan MAT. The results of C isotope variation were expressed as <sup>δ<sup>13</sup>C</sup> (‰) in relation to the standard Vienna Pee Dee Belemnite (VPDB) and those of nitrogen as <sup>δ<sup>15</sup>N</sup> (‰) in relation to atmospheric air, both with a precision of 0.2‰. The interpretation of the relationship between <sup>δ<sup>13</sup>C</sup> and <sup>δ<sup>15</sup>N</sup> was based on the data presented by Meyers (1994), Cloern et al. (2002), Ogrinc et al. (2005), and Miranda et al. (2009).

For <sup>14</sup>C dating of the soil OM, samples were collected at 40–50 cm for both soils, considering that the organic horizon of RJ-01 was 50 cm thick, and at 190–200 cm exclusively for RJ02. Only the humin fraction was used for this analysis because it is the most stable fraction of OM. The extraction method for the humin fraction was adapted from Gouveia et al. (1999). After extraction, the humin samples were sent to the <sup>14</sup>C Laboratory at the Center for Nuclear Energy in Agriculture (CENA) / USP for analysis by benzene synthesis and low-level liquid scintillation counting (Pessenda and Camargo, 1991). The <sup>14</sup>C conventional data is given in years before present (BP), corrected by isotope fractionation (-25‰), and calibrated (cal years BP) using CALIB 8.2 software (Stuiver et al., 2021) and with calibration curve SHcal20 with 95% probability and estimated error of 2σ (Hogg et al., 2020).

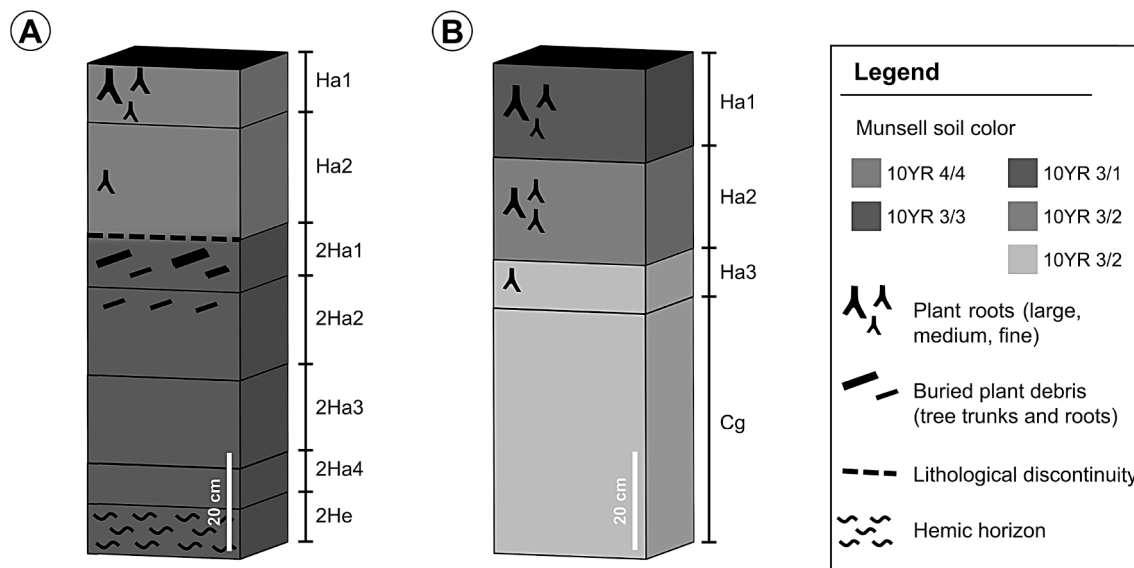


Fig. 2. Morphological characteristics of the studied soil (A) RJ-01, (B) RJ-02.

2.4. Statistical analysis

The results of the soil analyses were explored using descriptive statistical analysis (maximum, minimum, and mean). Principal component analysis (PCA) was performed using the XLStat software. For the PCA, the following morphological, physical, and chemical variables that had the highest weight and that best characterized each component were used: pH, S, T, RF, Bd, Pd, OMD, MR, OM, C, H, N, C-HUM, and C-HA. Diagrams were plotted using TILIA and TGView 1.7.16 and CONISS cluster analysis by similarity index to calculate the zone boundaries (Grimm, 1992).

3. Results

3.1. Soil morphology, physic and chemical characteristics

Both soils presented horizons with organic soil materials under conditions of saturation and reduction, characterizing a histic epipedon. In RJ-01, the thickness of the organic horizons exceeded 100 cm, while in RJ-02 it was 50 cm, followed by a subsurface mineral horizon (Cg) (Fig. 2; Table 2). Suffix symbols were used to indicate highly decomposed (a) and intermediate decomposition (e) of the organic materials in the organic horizons, and strong gleying (g) in the mineral horizon at the base of the RJ-02. In the organic horizons, these suffixes were defined

based on the values of the VP scale, RF, and PI.

In terms of soil colors, RJ-01 showed superficial horizons (Ha1 and Ha2) with lighter colors (10YR 4/4) than the deeper horizons (2Ha1 to 2He, 10YR 3/3). Plant remains (wood fragments and roots) were observed 35 cm deep in this pedon. The deepest sampled horizon (2He) differed from the others in that it presented hemic organic materials. In RJ-02, the surface horizon showed a darker color (10YR 3/1), becoming lighter in depth (10YR 3/2 in Ha2, and 10YR 6/1 in Ha3 and Cg). In this soil, a large number of plant roots were observed in the histic epipedon (Table 2; Fig. 2).

The soil structure was granular in the Ha1 and Ha2 horizons of both pedons, becoming massive (in the structural units; material is a coherent mass) in the deeper horizons. The percentage of rubbed fibers varied from 12% to 26% in RJ-01, increasing in depth, and from 12% to 20% in RJ-02, decreasing in depth. Except for the 2He horizon in RJ-01, all horizons presented sapric organic materials. The VP index varied from H7 to H9, and the PI ranged from 2 to 5.

Regarding chemical attributes, low pH values were found in the soils, ranging from 3.09 to 3.95 in RJ-01, and from 4.03 to 5.14 in RJ-02 (Table 3). In the Brazilian Soil Classification System (Sistema Brasileiro de Classificação de Solos – SiBCS) (Santos et al., 2018) and in the Soil Taxonomy (Soil Survey Staff, 2014), horizons with thickness ≥ 15 cm and pH (H<sub>2</sub>O) values lower than 3.5, are typical of sulfuric horizons, as shown in the RJ-01, classified in the level of suborder as Thiomorphic in

Table 2  
Morphological characteristics of the Histosols in floodplain environment of Rio de Janeiro State, Brazil.

Horizons	Depth (cm)	Color	Texture	Soil structure <sup>a</sup>	Von post		RF <sup>b</sup> %	PI <sup>c</sup>
					Index	Material		
<b>RJ-01 Typic Sulfosaprists</b>								
Ha1	0–12	10YR 4/4	organic	mod, m/l, gran.	H8	sapric	12	3
Ha2	12–35	10YR 4/4	organic	mod, m/l, gran.	H8	sapric	16	3
2Ha1	35–46	10YR 3/3	organic	massive	H8	sapric	17	3
2Ha2	46–64	10YR 3/3	organic	massive	H9	sapric	18	3
2Ha3	64–82	10YR 3/3	organic	massive	H9	sapric	18	2
2Ha4	82–90	10YR 3/3	organic	massive	H9	sapric	20	2
2He	90–100 <sup>+</sup>	10YR 3/3	organic	massive	H7	hemic	26	2
<b>RJ-02 Terric Haplosaprists</b>								
Ha1	0–19	10YR 3/1	organic	mod, s/m, gran.	H9	sapric	17	2
Ha2	19–40	10YR 3/2	organic	mod, s/m, gran.	H9	sapric	20	2
Ha3	40–50	10YR 6/1	organic	massive	H9	sapric	17	5
Cg	50–67 <sup>+</sup>	10YR 6/1	clay	massive			12	5

<sup>a</sup> Structure: mod: moderate; s: small; m: medium; l: large; gran: granular. <sup>b</sup>RF: rubbed fibers; <sup>c</sup>PI: pyrophosphate index.

**Table 3**  
Chemical characteristics of the Histosols in floodplain environment of Rio de Janeiro State, Brazil.

Horizons	pH	Ca	Mg	Al	H	Na	K	S <sup>a</sup>	T <sup>b</sup>	P	V% <sup>c</sup>	Na% <sup>d</sup>	m% <sup>e</sup>
		cmol <sub>c</sub> kg <sup>-1</sup>								mg kg <sup>-1</sup>			
<b>RJ-01 Typic Sulfosaprists</b>													
Ha1	3.70	1.5	0.3	1.6	15.9	0.6	0.4	2.8	20.3	1	13	3	8
Ha2	3.95	1.2	0.7	5.5	22.6	0.5	0.2	2.6	30.7	3	8	2	18
2Ha1	3.46	1.4	2.3	7.5	27.1	0.5	0.2	4.4	39.0	9	11	1	19
2Ha2	3.09	1.5	3.4	3.6	12.5	0.6	0.2	5.7	21.7	6	26	3	16
2Ha3	3.28	1.5	5.7	5.1	16.4	0.5	0.2	7.8	29.3	6	26	2	17
2Ha4	3.24	1.6	6.4	4.6	20.5	0.6	0.2	8.8	33.9	5	25	2	13
2He	3.84	0.7	3.2	5.0	19.3	0.4	0.1	4.3	28.6	10	15	1	18
<b>RJ-02 Terric Haplosaprists</b>													
Ha1	4.16	1.7	2.3	1.6	43.5	2.1	10.0	7.2	52.4	4	13	4	3
Ha2	4.03	3.3	3.8	1.3	44.2	2.3	11.0	9.7	55.2	2	17	4	2
Ha3	5.22	0.8	1.0	0.3	25.4	0.8	0.4	3.0	28.7	2	10	3	1
Cg	5.14	0.5	1.0	0.2	4.2	0.4	0.0	2.0	6.3	6	30	6	3

<sup>a</sup>S: sum of bases. <sup>b</sup>T: cation-exchangeable capacity. <sup>c</sup>V%: bases saturation. <sup>d</sup>Na%: exchangeable sodium percentage. <sup>e</sup>m%: aluminum saturation.

the SiBCS and as Sulfosaprists in the level of great group in the Soil Taxonomy. Santos et al. (2020) also observed the occurrence of peatlands with acid sulfate soils in a coastal environment in the State of Rio de Janeiro, in an area close to RJ-01.

The Al<sup>3+</sup> content was also high, resulting in m% of up to 19 (Ha3; RJ-01). In general, the content of exchangeable basic cations (Ca<sup>2+</sup>, Mg<sup>2+</sup>, and K<sup>+</sup>) was low, based on the S values, whose maximum, minimum, and mean were 9.7, 2.0, and 5.3 cmol<sub>c</sub> kg<sup>-1</sup>, respectively. The Ca<sup>2+</sup> content ranged from 0.5 cmol<sub>c</sub> kg<sup>-1</sup> (Cg; RJ-02) to 3.3 cmol<sub>c</sub> kg<sup>-1</sup> (Ha2; RJ-01). The Mg<sup>2+</sup> content ranged from 0.3 cmol<sub>c</sub> kg<sup>-1</sup> (Ha1; RJ-01) to 3.8 cmol<sub>c</sub> kg<sup>-1</sup> (Ha2; RJ-02), and the Mg<sup>2+</sup> content was higher than the Ca<sup>2+</sup> content, except for Ha1 and Ha2 of the RJ-01. Excluding horizons Ha1 and Ha2 of the RJ-02, the K<sup>+</sup> content was low, ranging from 0.0 to 0.4 cmol<sub>c</sub> kg<sup>-1</sup>.

In the RJ-01Na<sup>+</sup> contents showed low values, ranging from 0.4 to 0.6 cmol<sub>c</sub> kg<sup>-1</sup>, whereas these values were higher in the RJ-02, ranging from 0.4 to 2.3 cmol<sub>c</sub> kg<sup>-1</sup>, which provided higher ESP values, by up to 6%, as shown in Cg. The P content was also low, ranging from 1 to 10 mg kg<sup>-1</sup>, in horizons Ha1 and 2He, both in RJ-01, increasing with depth.

The T value ranged from 55.2 (Ha2; RJ02) to 6.3 cmol<sub>c</sub> kg<sup>-1</sup> (Cg; RJ-02) and were lower than those of other soils with high OM content (Ebeling et al., 2011; Cipriano-Silva et al., 2014; Santos et al., 2020). The V% values were also low, ranging from 8% to 30%, because the contribution of basic cations was smaller than that of H<sup>+</sup> (H + Al), characterizing both soils as dystrophic.

In the RJ-01, the highest Bd values were found in surface horizons (0.71 and 0.57 g cm<sup>-3</sup> for Ha1 and Ha2, respectively), decreasing in Ha3 and stabilizing up to 1 m. Conversely, in RJ-02, Bd increased with depth, peaking at 1.28 g cm<sup>-3</sup> in horizon Cg. The high value of Bd in Ha (0.73 g

cm<sup>-3</sup>) indicates that this horizon has a strong mineral fraction effect (Table 4).

The Pd values varied considerably between horizons within the same pedon, given the organic material composition, content, and characteristics of each horizon. Only the horizon Cg of RJ-02 showed Pd values higher than 2 g cm<sup>-3</sup>, due to the mineral material content. Low OMD values (Ebeling et al., 2013) were observed in both areas, ranging from 0.15 g cm<sup>-3</sup> (Ha; RJ-02) to 0.32 g cm<sup>-3</sup> (Ha2; RJ-01). The pedons had high MR values, ranging from 0.13 to 0.73 m m<sup>-1</sup>, identifying the latter in horizon Cg, in RJ-02.

The moisture content (Gh) varied with depth, especially in RJ-01, where the lowest values occurred in the first three horizons and in the last (2He); in contrast, in RJ-02, Gh tended to decrease with depth. In RJ-01, the TPV value showed an irregular pattern with depth, ranging from 30.4 to 65.3, with no direct relationship with Gh. In RJ-02, these values decreased with depth, with TPV ranging from 65.3 to 45.7%. In RJ-01, MM decreased with depth up to horizon 2Ha3 (38.0%), and subsequently increased again in 2He (52.7%). In RJ-02, the values increased with depth up to 86.1% in Cg, with distinct and inverse patterns between the pedons.

Based on the characterization and properties of the soils, the pedon RJ-01 was classified as Typic Sulfosaprists (*Organossolo Tiomórfico Sáprico típico*) and pedon RJ-02 as Terric Haplosaprists (*Organossolo Háptico Sáprico típico*).

### 3.2. Distribution of C, N, and carbon in humic fractions

The distribution patterns of C, H, and N in humic substances differed between the two areas (Table 5). The C content ranged from 1.27 to

**Table 4**  
Physical attributes and contents of organic matter (OM) in two Histosols of floodplain environment of Rio de Janeiro State, Brazil.

Horizontes	Bd <sup>a</sup>	Pd <sup>b</sup>	OMD <sup>c</sup>	MR <sup>d</sup>	GH <sup>e</sup>	TPV <sup>f</sup>	MM <sup>g</sup>	OM
	g cm <sup>-3</sup>			m m <sup>-1</sup>	%			
<b>RJ-01 Typic Sulfosaprists</b>								
Ha1	0.71	1.83	0.22	0.32	13.4	61.5	68.9	31.1
Ha2	0.57	1.50	0.32	0.16	41.8	62.0	43.3	56.7
2Ha1	0.48	0.30	0.29	0.13	22.7	61.5	39.3	60.7
2Ha2	0.51	1.44	0.30	0.15	68.6	64.3	42.5	57.5
2Ha3	0.51	0.74	0.30	0.14	83.8	30.4	41.0	59.0
2Ha4	0.52	1.15	0.32	0.13	73.6	55.1	38.0	62.0
2He	0.52	1.32	0.25	0.18	13.5	60.6	52.7	47.3
<b>RJ-02 Terric Haplosaprists</b>								
Ha1	0.56	1.54	0.23	0.22	17.3	65.3	59.2	40.8
Ha2	0.46	0.32	0.21	0.17	20.5	57.0	54.2	45.8
Ha3	0.73	1.84	0.15	0.38	12.0	52.1	79.0	21.0
Cg	1.28	2.33	0.18	0.73	11.8	45.7	86.1	13.9

<sup>a</sup>BD: bulk density. <sup>b</sup>PD: particle density. <sup>c</sup>OMD: organic matter density. <sup>d</sup>MR: minimal residue. <sup>e</sup>GH: gravimetric humidity, <sup>f</sup>TPV: Total Pore Volume. <sup>g</sup>MM: Mineral Material.

**Table 5**

Values of carbon (C), hydrogen (H), nitrogen (N) and C levels in the fractions of humic substances in two Histosols of floodplain environment of Rio de Janeiro State, Brazil.

Horizons	C %	H	N	C:N	H:C	C-HUM <sup>a</sup> g kg <sup>-1</sup>	C-HA <sup>b</sup>	C-FA <sup>c</sup>	C-HA/C-FA
<b>RJ-01 Typic Sulfosaprists</b>									
Ha1	10.87	2.75	0.60	18.1	0.25	163.13	10.85	12.10	0.90
Ha2	25.10	4.18	1.06	23.7	0.17	178.84	10.58	12.85	0.82
2Ha1	27.61	4.38	1.02	27.1	0.16	340.84	19.47	4.84	4.02
2Ha2	34.24	2.56	1.68	20.4	0.07	174.40	20.22	3.67	5.52
2Ha3	28.88	2.54	1.16	25.0	0.09	212.44	19.85	3.06	6.48
2Ha4	29.45	3.90	1.07	27.5	0.13	314.78	19.47	3.44	5.66
2He	21.16	3.38	0.63	33.6	0.16	151.16	9.34	3.48	2.68
<b>RJ-02 Terric Haplosaprists</b>									
Ha1	24.85	3.67	1.60	15.5	0.15	105.00	7.17	7.08	1.01
Ha2	35.95	4.47	1.93	18.6	0.12	116.39	7.28	4.47	1.62
Ha3	9.83	2.87	0.53	18.6	0.29	58.65	2.55	7.01	0.36
Cg	1.27	0.87	0.07	18.1	0.69	47.26	1.85	3.14	0.58

C:N and H:C Ratio. <sup>a</sup>C-HUM: C of humine. <sup>b</sup>C-HA: C of acid humic. <sup>c</sup>C-FA: C of acid fulvic.

35.95%, and these values tended to increase with depth in RJ-01, in contrast in RJ-02 where it tended to decrease with depth. The H and N contents showed small variations between the horizons in the two pedons, with maximum values of 4.47 and 0.87% and minimum values of 1.93 and 0.07%, respectively.

The values of the C:N ratio of RJ-01 were higher than those of RJ-02 and ranged from 18.1 to 33.6, whereas they ranged from 15.5 to 18.6 in RJ-02. All H:C contents were lower than 1, ranging from 0.07 to 0.69.

In relation to the chemical fractionation of humic substances, both pedons showed higher mean contents in the C-HUM fraction, followed by the C-HA and C-FA fractions. The C-HUM contents ranged from 47.26 to 340.84 g kg<sup>-1</sup>, which varied irregularly between the horizons of RJ-01, whereas the content decreased with depth in RJ-02. The maximum and minimum values of C-HA were 20.22 and 1.85 g kg<sup>-1</sup>, respectively, maintaining an irregular pattern between the RJ-01 horizons, similar to C-HUM. Conversely, in RJ-02, the C-HA content decreased as the depth increased. The C-FA content ranged from 12.85 to 3.06 g kg<sup>-1</sup> and tended to be higher at the surface. The values of the C-HA/C-FA ratio ranged from 6.48 to 0.36, with higher values in sub-surface horizons of the RJ-01 (2Ha1, 2Ha2, 2Ha3, 2Ha4), given the increase in C-FA at the surface (Ha1 and Ha2).

Principal component analysis showed that the first component (F1

axis) explained most of the variations observed (64.57%) and that the sum of the first two components (Axis F1 + F2) was 80.93% (Fig. 3). Most variables contributed to the increased variance of the first principal component, especially Bd, Pd, MR, C, and OM. The variable pH showed a negative correlation with C-HA, C-HUM, OMD, and OM, which in turn are strongly correlated with each other. The C content showed a negative correlation with Bd, Pd, and MR and a positive correlation with S, N, H, and RF, which in turn showed a strong positive correlation with each other (Fig. 3A).

When evaluating the spatial distribution of the points corresponding to the horizons in the F1 and F2 axes, the two pedons showed different patterns of distribution (Fig. 3B). The points corresponding to horizons from RJ-01 clustered in the third quadrant, with a lower correspondence only with Ha1 and 2He, which were the first and last horizons, respectively. The variables OM, C-HUM, C-HA, and OMD determined the behavior of these horizons. Conversely, the points corresponding to the horizons of RJ-02 are scattered, forming an elongated ellipse.

### 3.3. Elemental C and N, isotopic composition ( $\delta^{13}\text{C}$ and $\delta^{15}\text{N}$ ) and $^{14}\text{C}$ dating

The analysis of C and N up to 200 cm showed clear differences

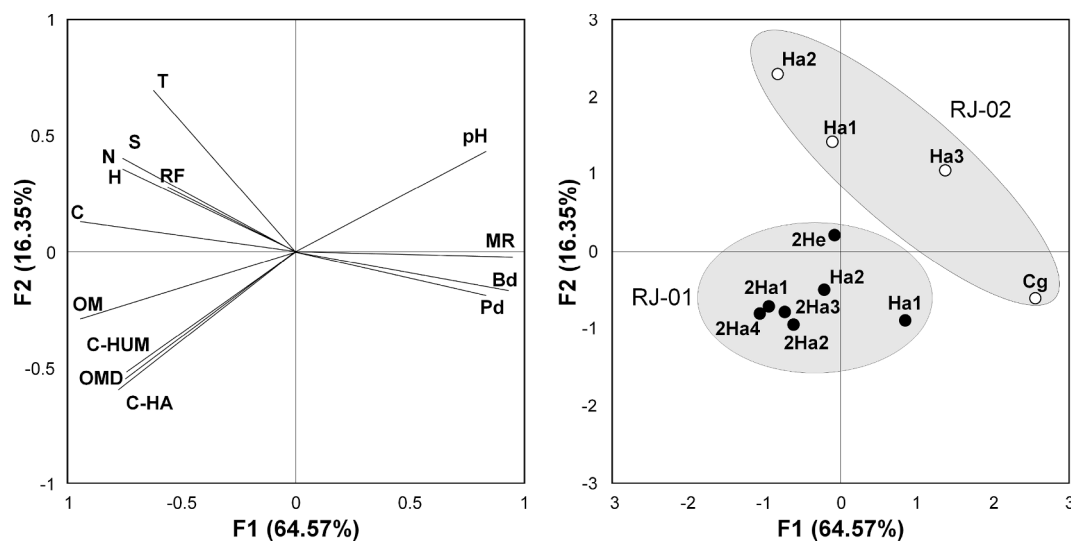


**Fig. 3.** Principal component analysis (PCA). A) Ordering diagram of the auto vectors of the variables: pH, sum of bases (S), cation-exchangeable capacity (T), percentage of rubbed fiber (RF), bulk density (Bd), particles density (Pd) and organic matter density (OMD), minimal residue (MR), organic matter (OM), carbon (C), hydrogen (H), nitrogen (N), C content of humine fraction (C-HUM) and humic acid fraction (C-HA). B) Diagram of ordering the horizons of the RJ-01 and RJ-02 pedons on the main axes.

between the two pedons (Fig. 4). In RJ-01, C increased until approximately 130 cm, the values of which were higher than 20%. After this depth, the values decrease slightly, remaining close to 15%.

Pedon RJ-02 showed the reverse pattern, in which C increased up to a depth of 40 cm, with values close to 20%. From 50 to 80 cm, C decreases sharply to values close to 3%, and from 80 cm onward, the values are closer to zero (null). This decrease in C with depth in RJ-02 is associated with the transition of an organic (Ha) to a mineral horizon (Cg). N showed a pattern similar to that of C in both pedons. In RJ-01, N increases up to approximately 1.4% at a depth of 40 cm, remaining close to 1% until 140 cm, and decreasing to approximately 0.5% up to 200 cm. In RJ-02, the initial values were higher, close to 1.5% up to 40 cm, decreasing to 0.5% between 40 and 70 cm, and becoming virtually null after 80 cm, where the mineral material prevails. In RJ-01, the values of C/N increased with depth (18.1, from Ha1 to 33.6, in 2He). In contrast, in RJ-02, the values remained close to 10 throughout the pedon.

In RJ-01, the  $\delta^{13}\text{C}$  values showed small variations with depth, ranging from  $-27$  to  $-29\text{‰}$ . From 90 to 120 cm, the  $\delta^{13}\text{C}$  varied from  $-27.03$  to  $-28.6\text{‰}$ . In RJ-02,  $\delta^{13}\text{C}$  values varied from  $-25.98\text{‰}$  at the surface up to  $-27.61\text{‰}$  at 30 cm, varying to  $-26.11\text{‰}$  at 60 cm, to  $-29.48\text{‰}$  at 90 cm, and to  $-30.57\text{‰}$  from 150 to 200 cm. Regarding  $\delta^{15}\text{N}$  values, both pedons show small variation with depth, ranging from 2 to 5‰, except for RJ01, whose  $\delta^{15}\text{N}$  varied up to 10‰ (130 cm) to  $-2.5\text{‰}$  (140 cm). The relationships between  $\delta^{13}\text{C}$  and  $\delta^{15}\text{N}$ , and C/N and  $\delta^{13}\text{C}$  showed different patterns between the two soils (Fig. 5A and 5B, respectively).

The relationship between C/N and  $\delta^{13}\text{C}$  (Fig. 3B) indicates a predominance of  $\text{C}_3$  plants at the base of the RJ-01 pedon (200–90 cm), with dissolved organic carbon (DOC) contribution from 80 cm to the top of the profile. In RJ-02, the sources of organic matter appeared to be a mixture of  $\text{C}_3$  plants and DOC. The  $^{14}\text{C}$  dating of the humin fraction recorded ages of  $\sim 3938$  cal yr BP (190–200 cm) and  $\sim 2330$  cal years BP (40–50 cm) at RJ-01, and  $\sim 2009$  CE (40–50 cm) at RJ-02 (Table 6).

## 4. Discussion

### 4.1. Pedological processes

Significant variations in morphological properties, such as thickness, color, and fiber content, showed a relationship with chemical and physical soil properties. In turn, they are also related to the hydric and sedimentation dynamics responsible for the formation of deposits of organic material and soil formation. According to Clymo (1984), peat formation is characterized by three processes: i) partial decomposition of organic matter, release of  $\text{CO}_2$ , and leaching; ii) loss of physical structure; and iii) alteration of the chemical composition, characterized mainly by humification.

The coastal floodplains of Rio de Janeiro State are characterized by river, marine, or river–lake Quaternary sediments (Dantas et al., 2001). In depressions with water saturation and oxygen deficiency, the environment is reduced (Clymo, 1984), where organic matter accumulates through slow humification. In these environments, the genesis of Histosols is the result of a sequence of geogenic and pedogenic processes: (1) terrestrialization, when a depression (e.g., a lake) is filled with aquatic and/or terrestrial organic materials, such as plant residues (Clymo, 1984); (2) paludization, that is, the colonization of poorly drained land by plants (Pereira et al., 2005; van Breemen and Buurman, 2002; Buol et al., 2011; Silva Neto et al., 2019).

Pedon RJ-01 showed an alteration in the process of formation and/or deposition of organic matter in the peat at 35 cm depth, marked by a change in color (10YR 4/4 in Ha2 to 10YR 3/3 in 2Ha1) and in the soil structure (granular in Ha2 to massive in 2Ha1). In addition, on the 2Ha1 horizon, plant fragments (wood and roots) were found, indicating that it is a buried horizon. Another distinctive feature observed in this pedon was the presence of a hemic horizon (2He) at 90–100 cm depth. These features can be attributed to changes in the sedimentation process and water table fluctuation. According to Clymo (1984), these substantial changes can be due to the species composition of peat and widespread changes in vegetation, which over time results in changes that appear in

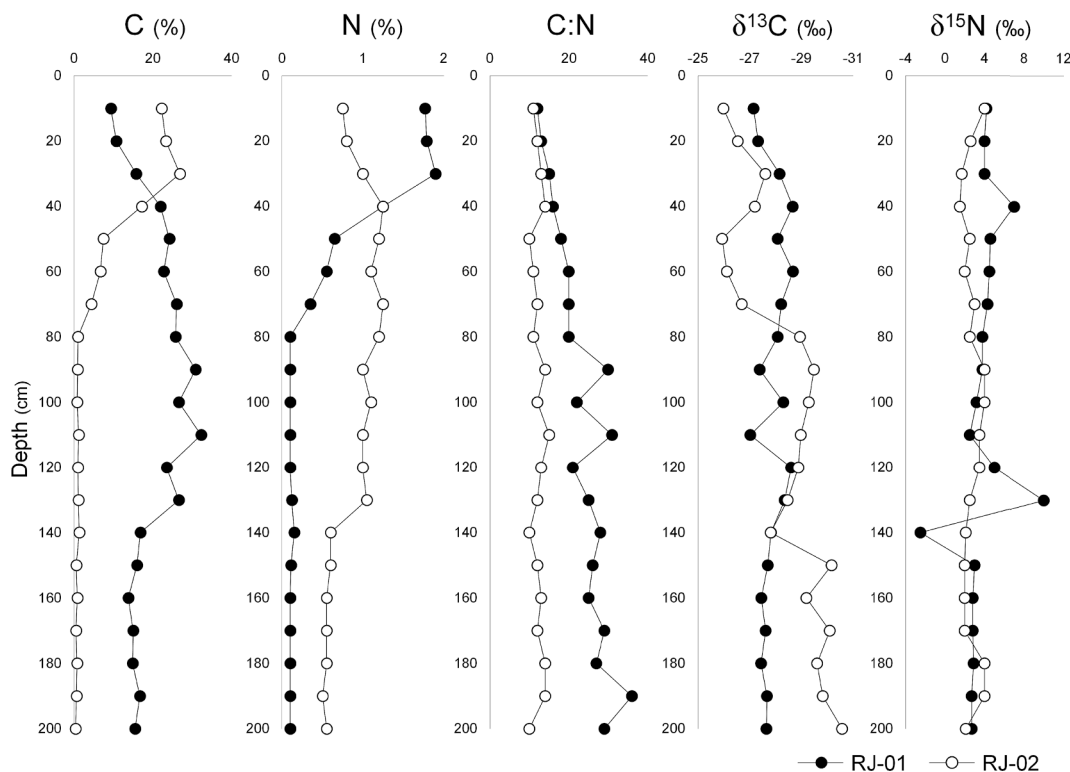
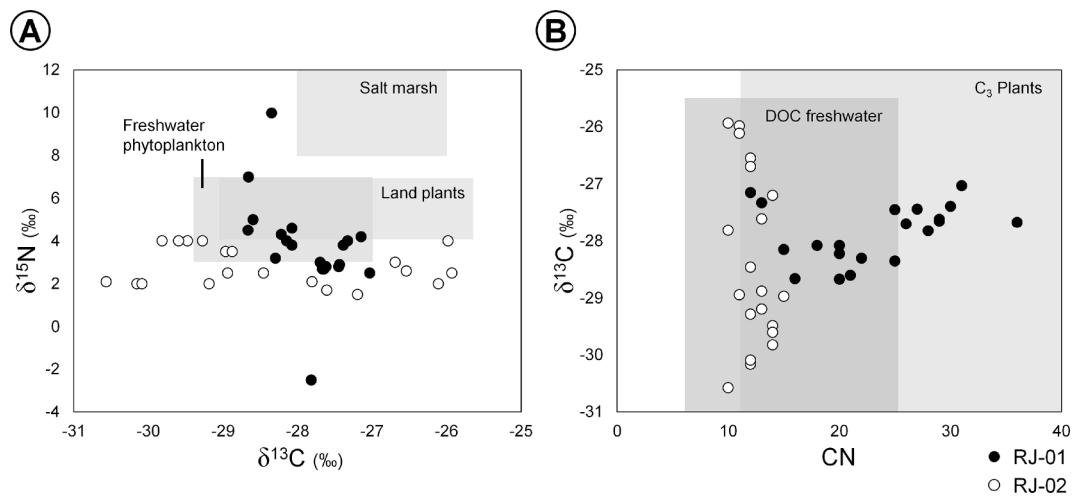


Fig. 4. Distribution of Carbon and Nitrogen content, C:N ratio and  $\delta^{13}\text{C}$  and  $\delta^{15}\text{N}$  of the studied pedons (RJ-01 and RJ-02).



**Fig. 5.** Relationship between  $\delta^{13}\text{C}$  and  $\delta^{15}\text{N}$  (A) and  $\delta^{13}\text{C}$  and C:N (B) of the studied pedons (RJ-01 and RJ-02). The interpretation of different grey boxes was based according to data presented by Meyers (1994), Cloern et al. (2002), Ogrinc et al. (2005) and Miranda et al. (2009).

**Table 6**

$^{14}\text{C}$  dating of the humin fraction from two profiles collected in floodplain environment of Rio de Janeiro State, Brazil.

Profile	Depth (cm)	Age (years BP) <sup>a</sup>	Calibrated age (years BP)	Mean calibrated age (years BP)
RJ-01	40–50	2310 ± 80	2121–2539	2330
	190–200	3640 ± 80	3720–4157	3938
RJ-02	40–50	Modern	2006–2012	2009

<sup>a</sup> Conventional  $^{14}\text{C}$  age (Before Present - BP, P = 1950).

the stratigraphy as quite abrupt transitions.

The pedon RJ-02 showed less thickness of organic horizons with a mineral horizon at a depth of 50 cm (Cg). Both soils presented a granular structure in the superficial horizons and a massive structure in the sub-superficial horizons. A granular structure is formed in surface horizons due to the effect of wetting and drying cycles, conditioned by drainage and/or agricultural use, and has also been assessed in other Histosols (Ebeling et al., 2013; Cipriano-Silva et al., 2014; Silva Neto et al., 2019; 2020).

The massive structure present in the deepest horizons (Cg) indicates that the water table had a strong influence, which is a limiting condition for the formation of well-defined soil aggregates (Silva Neto et al., 2019), since the formation of aggregates depends on alternating wetting and drying cycles. In historic horizons, the anaerobic conditions provided by the water table reduce the rate of decomposition of organic matter. The characteristics of the mineral horizon (Cg, pedon RJ-02) indicate the pedogenic process of gleization (van Breemen and Buurman, 2002; Buol et al., 2011). This process is characterized by the reduction of  $\text{Fe}^{3+}$  to  $\text{Fe}^{2+}$  by anaerobic microorganisms in the presence of SOM, primarily due to the presence of stagnant water. Consequently, low chroma, which is usually a grayscale color related to the mineral matrix of the soil, have been developed.

The physical and chemical characteristics of both soils showed high acidity due to the predominance of  $\text{H}^+$  ions in the sorption complex, due to the ionization of organic acids (RJ-01 and RJ-02) (Table 3). Notwithstanding the high values of  $\text{Al}^{3+}$ , the methods used to determine these values may overestimate the contents of this ion in soils with high OM content (Campos et al., 2014). This pattern of high acidity (lower pH) and an increase in  $\text{H}^+$  and  $\text{Al}^{3+}$  contents which were negatively correlated with OM levels, was also observed in other Histosols (Campos et al., 2010; Cipriano-Silva et al., 2014; Bispo et al., 2015; Silva Neto et al., 2019).

The lowest values of C in the surface horizons of both soils may be

related to modifications caused by the process of subsidence, with increased oxidation of labile organic matter and decreased C content. Bd and Pd values were negatively correlated with OM and C values (Fig. 3A), typical of histic horizons (Ebeling et al., 2013; Cipriano-Silva et al., 2014). The MR value is an estimate of the proportion between the residual and the original thickness of the histic horizons (Ebeling et al., 2013), which is positively correlated with Bd and Pd, indicating that the three variables are related to the subsidence of horizons with high levels of OM, thus corroborating the findings of Cipriano-Silva et al. (2014), who characterized Histosols in the Northeast region of Brazil.

Multivariate analysis (PCA; Fig. 3) allowed for the reduction and prediction of the set of variables that correlated. The pedons differ from each other in terms of their physical and chemical attributes, forming two distinct groups. The horizons of RJ-01 are more similar to each other and are related to OM content, OMD, C-HUM, and C-HA contents, and to the variable pH in the opposite quadrant, possibly associated with thiomorphism. Furthermore, OMD is an indicator of the extent to which organic matter is transformed (Lynn et al., 1974), and for that reason, it is related to the components of SH and the higher humification degree of OM. The 2He horizon is less similar, most likely due to the higher RF content, as is the Ha1 horizon, owing to its Bd and Pd values. Conversely, the horizons of RJ-02 are scattered, and the Cg horizon is related to the Bd, Pd, and MR values because this is a mineral horizon. The surface horizons Ha1 and Ha2 stand out for the high T and S values, probably due to nutrient cycling and intense bioturbation by plant roots (Boulet et al., 1995).

#### 4.2. Environmental interpretation

Through elementary analyses (C, N, and C: N ratios) in association with isotopic data ( $\delta^{13}\text{C}$  and  $\delta^{15}\text{N}$ ) and  $^{14}\text{C}$  dating, it was possible to establish three intervals that reflect the environmental changes in the studied floodplain environments (Fig. 6).

**Evaluation of pedon RJ-01:** At a depth of 200–120 cm, the values of  $\delta^{13}\text{C}$  and  $\delta^{15}\text{N}$  indicate a predominance of phytoplanktonic organic matter with the influence of terrestrial vegetation, suggesting the presence of vegetation composed predominantly of  $\text{C}_3$  vascular plants (Deines, 1980; Meyers, 1994; Cloern et al., 2002; Ogrinc et al., 2005; Miranda et al., 2009). In the 110–50 cm depth, is marked by a change in sedimentary deposition (2Ha1) until the organic horizon with hemic materials (high fiber content), 2He. In this pedon, this interval is characterized by a general increase in the C contents ( $26.9 \pm 2.7\%$ ), oscillation of the C:N ratio (31 to 18, mean =  $23 \pm 4.2$ ),  $\delta^{13}\text{C}$  ( $-27.03$  to  $-28.67$ , mean =  $-27.97 \pm 0.43\%$ ) at the bottom of the range, and a

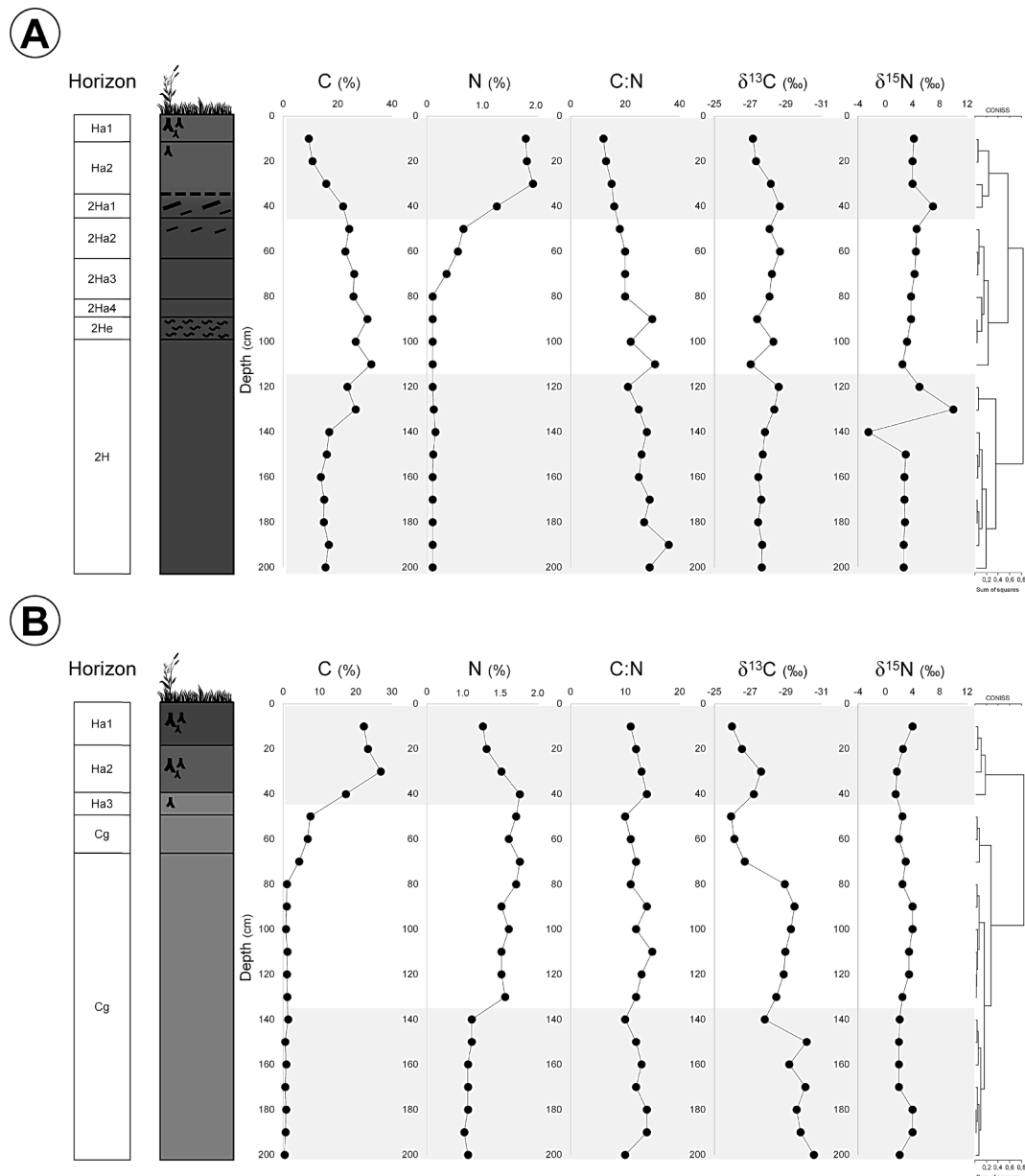


Fig. 6. C and N contents, C:N ratio and  $\delta^{13}\text{C}$  and  $\delta^{15}\text{N}$  of the studied soil (A) RJ-01, (B) RJ-02. White and gray horizontal bars indicate zones generated by CONISS.

trend of increase (from bottom to the top) in the N values (0.10 to 0.65, mean  $0.28 \pm 0.20\%$ ). These results, linked to the morphological, physical, and chemical characteristics of the soil, suggest the influence of alluvial sediments with subsequent stabilization of the soil surface. The irregular variation in the percentage of mineral material (38.0 to 52.7%), particle density ( $0.30$  to  $1.44 \text{ g cm}^{-3}$ ), and also in the carbon of humic fractions (Table 5) indicate the deposition of alluvial sediments transported by the Suruí River. Subsequently, the process of paludization, that is, the colonization of poorly drained land by plants, would have occurred approximately 2333 cal yr BP. A vegetation composed of  $\text{C}_3$  vascular plants was established in this area, as indicated by the presence of buried plant fragments (tree trunks and roots) in the 2Ha1 and 2Ha2 horizons.

Along the coast of Rio de Janeiro State, several authors have identified records of climatic oscillations that were responsible for the construction of the current coastal floodplain environments (e.g., Castro et al., 2014; Cunha et al., 2017; Jesus et al., 2017). In the coastal plains of Espírito Santo State, several studies have indicated the occurrence of

sedimentary deposits accumulated during the various stages of quaternary evolution, in marine terraces, as well as fluvio-marine, lagoon, and eolian environments (e.g., Buso Junior et al., 2013; França et al., 2015; Lorente et al., 2014). In the coastal plains of the São Paulo State, there are also studies indicating the formation of soils from river, marine, or river-lake Quaternary sediments, with grasslands and/or woodland vegetation, in soils subjected to hydromorphic conditions, such as Histosols and Spodosols (Rossi and Queiroz Neto, 2011; Coelho et al., 2010). Thus, the results observed in RJ-01 are related to the characteristics of coastal depositional environments associated with climatic, depositional, and vegetation dynamics during soil formation.

**Evaluation of RJ-02:** In this pedon, at 200 to 140 cm depth, the relationship between  $\delta^{13}\text{C}$  and  $\delta^{15}\text{N}$  seems to indicate a greater contribution of terrestrial plants and the interval corresponds to sediments deposited in the terrestrialization process during peat formation, with a lake being filled with a mixture of aquatic and terrestrial organic matter (Miranda et al., 2009; Zinck, 2011; Silva Neto et al., 2019). In the next section (130–50 cm) of this pedon, which comprises the horizons Ha3

and Cg, from the soil morphological description, the modern age obtained by  $^{14}\text{C}$  dating may be due to erosion processes and/or bioturbation during soil formation (Boulet et al., 1995). Variations in C:N ratios have been used to determine historical changes and mixtures in sources of organic matter because algae have a C:N ratio between 4 and 10, whereas terrestrial organic matter has a C:N ratio greater than 20 (Deines, 1980; Meyers, 1994). Decreases in C:N ratios have been used to identify periods when the environment has received a high proportion of algal organic matter (Kaushal and Binford, 1999). Similar results were reported by Silva Neto et al. (2019), who studied the genesis of Histosols under waterlogged conditions.

In both pedons, in the 0–40 cm layer, the  $\delta^{13}\text{C}$  and  $\delta^{15}\text{N}$  values suggest a mixture of algae and continental/terrestrial organic matter, which is also supported by the C:N values (Deines, 1980; Meyers, 1994; Miranda et al., 2009). The decrease in the contents of C and N in the superficial layer (0–10 cm) in both studied soils is probably indicative of the process of subsidence, which involves the reduction of bulk density, by the oxidation of organic matter (Cipriano-Silva et al., 2014). Changes in the hydrological characteristics of these soils that may lower the humidity content of the soil will eventually lead to the contraction of the volume of peatland, which is worsened by the oxidation and mineralization of the organic matter (Santos et al., 2020).

In terms of soil formation, the studied soils are linked to high contents of organic matter and processes of accumulation and redistribution of sulfates. Coastal environments are well-known for their important role in sulfur's geochemical cycle, conditions there are suitable to the formation and accumulation of sulfidric materials, mainly because of the abundant supply of sulfate from marine water and organic matter from the vegetation (Ferreira et al., 2007a,b). This may explain the high  $\text{Na}^+$  content in the Cg horizon. Under hydromorphic conditions, the partial pressure of  $\text{O}_2$  and the redox potential (Eh) of the soil were reduced. Consequently, other elements (such as sulfur in  $\text{SO}_4^{2-}$ ) are used as electron receptors to oxidize organic matter by anaerobic microorganisms during their respiratory processes. During this process, most of the sulfide generated reacts with reduced forms of iron ( $\text{Fe}^{2+}$ ) formed by the gleization process, and precipitates as iron sulfides, which may result in the formation of low-stability minerals, or even the synthesis of pyrite ( $\text{FeS}_2$ ), which is considered to be the end and more stable product of this process (Vidal-Torrado et al., 2010).

In the tropics, peatlands are subject to consistently warm and often humid conditions. Although elevated temperatures facilitate microbial decomposition and rapid turnover of OM, these parameters also increase the addition of OM due to longer growing seasons and associated higher local precipitation (Baker et al., 2016). Because peat accumulates when addition outstrips the decomposition of OM, the dominant control over peatland formation is the extent of flooding (Clymo, 1984). Water-logging enables anaerobic depositional conditions to prevail, which ultimately retards the rate of decomposition and permits the accumulation of OM-rich peat sediments. Although air temperature and local precipitation determine the rate of OM addition, microbial activity is also influenced by OM chemistry and reactivity, soil pH, redox conditions, and accessibility to potential decomposers (Schmidt et al., 2011; Baker et al., 2016).

In summary, the studied soils were characterized by organic matter of very similar origin, but they had different formation processes. Our results show that the occurrence of Histosols in coastal plains in Rio de Janeiro is related to drainage conditions that keep the environment permanently hydromorphic. This organic soil is formed by a combination of two processes: terrestrialization (accumulation of vegetable organic material in a lake depression) and paludization (colonization of the organic and poorly drained substrate by plants). Elementary (C and N) and isotopic ( $\delta^{13}\text{C}$  and  $\delta^{15}\text{N}$ ) analyses are useful tools to characterize the sources of organic matter (peat), the parent material of Histosols, which have a great influence on the soil properties.

## 5. Conclusions

An interproxy approach combining pedological analyses, radiocarbon dating, and elemental and isotopic analyses of total carbon and nitrogen of organic matter points out that the source material of these pedons consists of a mixture of algae and continental/terrestrial organic matter deposited in floodplain coastal environments (peatlands), at least ~ 4000 cal yr BP. The studied soils were formed by geogenic and pedogenic processes (terrestrialization, paludization, and aggradation). Considering the relationships between  $\delta^{13}\text{C}$  and  $\delta^{15}\text{N}$ , C/N and  $\delta^{13}\text{C}$ , and the soil characteristics, these deposits were probably formed by vertical accretion in lake environments. However, nearly 2300 cal yr BP, radiocarbon dating and isotopic data suggest the occurrence of deposition of alluvial sediments probably transported by the Suruí River in RJ-01. It is likely that the modern age obtained by  $^{14}\text{C}$  dating in RJ-02, dating near 3600 cal yr BP, is probably due to the intense bioturbation by plant roots and the input of young material by the erosional process.

## Declaration of Competing Interest

The authors declare that they have no known competing financial interests or personal relationships that could have appeared to influence the work reported in this paper.

## Acknowledgements

Authors thanks to FAPERJ, CAPES and CNPq for funded and support the fellowship.

## References

- Alvares, C.A., Stape, J.L., Sentelhas, P.C., Gonçalves, J.L.M., Sparovek, G. 2013. Köppen's climate classification map for Brazil. *Meteorol. Z.* 22, 711–728. <https://doi.org/10.1127/0941-2948/2013/0507>.
- Amador, E.S., 1997. Baía de Guanabara e Ecossistemas Periféricos: Homem e Natureza. E.S. Amador, Rio de Janeiro, p. 539.
- Andrieuse, J., 1988. Nature and management of tropical peat soils. In: *Bulletin Soils*, 59. FAO, Roma, p. 165.
- Baker, A., Routh, J., Roychoudhury, A.N., 2016. Biomarker records of palaeoenvironmental variations in subtropical Southern Africa since the late Pleistocene: Evidences from a coastal peatland. *Palaeogeogr. Palaeoclimatol. Palaeoecol.* 451, 1–12. <https://doi.org/10.1016/j.palaeo.2016.03.011>.
- Bispo, D.F.A., Silva, A.C., Christofaro, C., Silva, M.L.N., Barbosa, M.S., Silva, B.P.C., Barral, U.M., 2015. Characterization of headwaters peats of the Rio Araçuaí, Minas Gerais State. *Brazil. Rev. Bras. Ciênc. Solo* 39 (2), 475–489. <https://doi.org/10.1590/01000683rbc20140337>.
- Boulet, R., Pessenda, L.C.R., Telles, E.C.C., Melfi, A.J., 1995. Une évaluation de la vitesse de l'accumulation de matière par la faune du sol. Exemple des Latosols de versantes du lac Campestre, Salitre, Minas Gerais, Brésil. *Paris. C. R. Acad. Sci.* 320, 287–294.
- Breemen, N., Buurman, P., 2002. *Soil formation*, 2nd ed. Kluwer Academic Publishers, Dordrecht, p. 404p.
- Buol, S.W., Southard, R.J., Graham, R.C., McDaniel, P.A., 2011. *Soil genesis and classification*, 6th ed. John Wiley & Sons, Hoboken, p. 505.
- Buso Junior, A.A., Pessenda, L.C.R., de Oliveira, P.E., Giannini, P.C.F., Cohen, M.C.L., Volkmer-Ribeiro, C., Borotti Filho, M.A., 2013. From an estuary to a freshwater lake: a paleo-estuary evolution in the context of Holocene sea-level fluctuations, southeastern Brazil. *Radiocarbon* 55 (2–3), 1735–1746. <https://doi.org/10.1017/S0033822200048657>.
- Campos, J.R.D.R., Silva, A.C., Vasconcellos, L.L., Silva, D.V., Romão, R.V., Silva, E.D.B., Graziotti, P.H., 2010. Pedochronology and development of peat bog in the environmental protection area Pau-de-Fruta-Diamantina, Brazil. *Rev. Bras. Ciênc. Solo* 34 (6), 1965–1975. <https://doi.org/10.1590/S0100-06832010000600021>.
- Campos, J.R.d.R., Silva, A.C., Silva, E.d.B., Vidal-Torrado, P., 2014. Extração e quantificação de alumínio trocável em Organossolos. *Pesq. Agropec. Bras.* 49 (3), 207–214. <https://doi.org/10.1590/S0100-204X2014000300007>.
- Castro, J.W.A., Suguio, K., Seoane, J.C.S., Cunha, A.M., Dias, F.F., 2014. Sea-level fluctuations and coastal evolution in the state of Rio de Janeiro, southeastern Brazil. *Anais da Academia Brasileira de Ciências* 86 (2), 671–683.
- Cipriano-Silva, R., Valladares, G.S., Pereira, M.G., Anjos, L.H.C.D., 2014. Caracterização de Organossolos em ambientes de várzea do Nordeste do Brasil. *Rev. Bras. Ciênc. Solo* 38 (1), 26–38. <https://doi.org/10.1590/S0100-06832014000100003>.
- Cloern, J.E., Canuel, E.A., Harris, D., 2002. Stable carbon and nitrogen isotope composition of aquatic and terrestrial plants of the San Francisco Bay estuarine system. *Limnol. Oceanog.* 47 (3), 713–729. <https://doi.org/10.4319/lo.2002.47.3.0713>.

- Clymo, R.S., 1984. The limits to peat bog growth. *Philos. Trans. the Royal Soc. London B, Biol. Sci.* 303 (1117), 605–654. <https://doi.org/10.1098/rstb.1984.0002>.
- Coelho, M.R., Martins, V.M., Vidal-Torrado, P., Souza, C.R.G., Perez, X.L.O., Vásquez, F. M., 2010. Relação solo-relevo-substrato geológico nas restingas da planície costeira do estado de São Paulo. *R. Bras. Ci. Solo* 34, 833–846. <https://doi.org/10.1590/S0100-06832010000300025>.
- Costa, L.A.A., Pessoa, D.M.M., Carreira, R.S., 2018. Chemical and biological indicators of Sewage River input to an urban tropical estuary (Guanabara Bay, Brazil). *Ecol. Indic.* 90, 513–518. <https://doi.org/10.1016/j.ecolind.2018.03.046>.
- Cunha, A.M., Castro, J.W.A., Pereira, F.M.B., Carvalho, M.A., Suguio, K., 2017. Variações do nível relativo do mar durante o Holoceno na bacia hidrográfica do rio Uma, registro de Cabo Frio – Rio de Janeiro: aspectos sedimentológicos, faciologicos e geocronológicos. *Revista Brasileira de Geomorfologia* 8, 143–154.
- Dantas, M.E., Shinzato, E., Medina, A.I.D.M., Silva, C.R.D., Pimentel, J., Lumbrellas, J.F., Calderano, S.B., Carvalho Filho, A.D., 2001. Diagnóstico geoambiental do estado do Rio de Janeiro - Estudo geoambiental do estado do Rio de Janeiro. Serviço Geológico do Brasil, Brasília - DF 33.
- Deines, P., 1980. The isotopic composition of reduced organic carbon. In: Fritz, P., Fontes, J.C. (Eds.), *Handbook of Environmental Isotope Geochemistry. The Terrestrial Environments*, Elsevier, Amsterdam, pp. 329–406.
- Ebeling, A.G., Anjos, L.H.C.D., Perez, D.V., Pereira, M.G., Gomes, F.W.d.F., 2011. Atributos químicos, carbono orgânico e substâncias húmicas em Organossolos Háplicos de várias regiões do Brasil. *Rev. Bras. Ciênc. Solo* 35 (2), 325–336. <https://doi.org/10.1590/S0100-06832011000200004>.
- Ebeling, A.G., Anjos, L.H.C.D., Pérez, D.V., Pereira, M.G., Novotny, E.H., 2013. Atributos físicos e matéria orgânica de Organossolos Háplicos em distintos ambientes no Brasil. *Rev. Bras. Ciênc. Solo* 37 (3), 763–774. <https://doi.org/10.1590/S0100-06832013000300023>.
- Ferreira, T.O., Otero, X.L., Vidal-Torrado, P., Macías, F., 2007a. Redox processes in mangrove soils under in relation to different environmental conditions. *Soil Sci. Soc. Am. J.* 71, 484. <https://doi.org/10.2136/sssaj2006.0078>.
- Ferreira, T.O., Vidal-Torrado, P., Otero, X.L., Macías, F., 2007b. Are mangrove forest substrates sediments or soils? A case study in southeastern Brazil. *Catena* 70 (1), 79–91. <https://doi.org/10.1016/j.catena.2006.07.006>.
- França, M.C., Alves, I.C.C., Castro, D.F., Cohen, M.C.L., Rossetti, D.F., Pessenda, L.C.R., Lorente, F.L., Fontes, N.A., Junior, A.Á.B., Giannini, P.C.F., Francisquini, M.I., 2015. A multi-proxy evidence for the transition from estuarine mangroves to deltaic freshwater marshes, Southeastern Brazil, due to climatic and sea-level changes during the late Holocene. *Catena* 128, 155–166.
- Gouveia, S.E.M., Pessenda, L.C.R., Aravena, R., 1999. Datação da fração húmica da matéria orgânica do solo e sua comparação com idades  $^{14}\text{C}$  de carvões fósseis. *Quim. Nova* 22, 810–814. <https://doi.org/10.1590/S0100-40421999000600007>.
- Grimm, E.C., 1992. Tilia and Tilia-Graph: pollen spreadsheet and graphics programs. Abstracts 8th International Palynological Congress. Aix-en-Provence: 56.
- Gumbrecht, T., Roman-Cuesta, R.M., Verchot, L., Herold, M., Wittmann, F., Householder, E., Herold, N., Muriyasar, D., 2017. An expert system model for mapping tropical wetlands and peatlands reveals South America as the largest contributor. *Global Change Biol.* 23 (9), 3581–3599. <https://doi.org/10.1111/gcb.2017.23.issue-910.1111/gcb.13689>.
- Hogg, A.G., Heaton, T.J., Hua, Q., Palmer, J.G., Turney, C.S.M., Southon, J., Bayliss, A., Blackwell, G.P., Boswijk, G., Ramsey, B.C., Pearson, C., Petchev, F., Reimer, P., Reimer, R., Wacker, L., 2020. SHCal20 Southern Hemisphere calibration, 0–55,000 years cal BP. *Radiocarbon* 62 (4), 59–778. <https://doi.org/10.1017/RDC.2020.59>.
- IBGE, Divisão Territorial do Brasil e Limites Territoriais. Instituto Brasileiro de Geografia e Estatística (IBGE), 2008. Acessado em: 28 de fevereiro de 2021.
- Jesus, P.B., Dias, F.F., Muniz, R.A., Macário, K.C.D., Seoane, C.S., Quattrociochi, D.G.S., Cassab, R.C.T., Aguilera, O., Souza, R.C.C.L., Alves, E.Q., Chanca, I.S., Carvalho, G.R. A., Araujo, J.C., 2017. Holocene paleo-sea level in southeastern Brazil: an approach based on vermetid shells. *J. Sedimentary Environ.* 2 (1), 35–48. <https://doi.org/10.12957/jse.2017.28158>.
- Junk, Wolfgang J., An, Shuqing, Finlayson, C.M., Gopal, Brij, Květ, Jan, Mitchell, Stephen A., Mitsch, William J., Robarts, Richard D., 2013. Current state of knowledge regarding the world's wetlands and their future under global climate change: A synthesis. *Aquat. Sci.* 75 (1), 151–167. <https://doi.org/10.1007/s00027-012-0278-z>.
- Kaushal, S., Binford, M.W., 1999. Relationship between C:N ratios of lake sediments, organic matter sources, and historical deforestation in Lake Pleasant, Massachusetts, USA. *J. Paleolimnol.* 22 (4), 439–442.
- Lamb, Angela L., Wilson, Graham P., Leng, Melanie J., 2006. A review of coastal palaeoclimate and relative sea-level reconstructions using  $\delta^{13}\text{C}$  and C/N ratios in organic material. *Earth-Sci. Rev.* 75 (1–4), 29–57. <https://doi.org/10.1016/j.earscirev.2005.10.003>.
- Lemos, R.M.J., 2002. *Leitura Histórica do Processo de Apropriação do Território – um estudo no município de Magé - RJ. XIII Encontro da Associação Brasileira de Estudos Populacionais. Ouro Preto, Minas Gerais.*
- Lima, V.S., Nascimento, F.H., Nascentes Coelho, A.L., Miro, J.M.R., 2013. Análise de áreas sazonalmente inundáveis com uso de técnicas de sensoriamento remoto: o caso da Lagoa Feia, região Norte do estado do Rio de Janeiro. *Anais XVI Simpósio Brasileiro de Sensoriamento Remoto - SBSR, Foz do Iguaçu, Brasil.*
- Lorente, F.L., Pessenda, L.C.R., Oboh-Ikenobé, F., Buso Júnior, A.A., Cohen, M.C.L., Meyer, K.E.B., Giannini, P.C.F., Oliveira, P.E., Rossetti, D.F., Borotti Filho, M.A., França, M.C., Ferreira, Darcilêa, de Castro, D.F., Bendassolli, J.A., Kita Macario, K., 2014. Palynofacies and stable C and N isotopes of Holocene sediments from Lake Macuco (Linhares, Espírito Santo, southeastern Brazil): Depositional settings and palaeoenvironmental evolution. *Palaeogeogr. Palaeoclimatol. Palaeoecol.* 415, 69–82. <https://doi.org/10.1016/j.palaeo.2013.12.004>.
- Luz, C.F., Barth, O.M., Martín, L., Silva, C.G., Turcq, B.J., 2011. Palynological evidence of the replacement of the hygrophilous forest by field vegetation during the last 7,000 years BP in the northern coast of Rio de Janeiro, Brazil. *Anais da Academia Brasileira de Ciências* 83 (3), 939–952. <https://doi.org/10.1590/S0001-37652011005000031>.
- Lynn, W.C., Mckinze, W.E., Grossman, R.B. 1974. Field laboratory test for characterization of Histosols. In: STELLY, M., ed. *Histosols: their characteristics and use*. Madison, Soil Science Society of America (SSSA Special Publication Series, 6), p. 11–20. Doi: 10.2136/sssaspepub6.c2.
- Miranda, M.C.D.C., Rossetti, D.D.F., Pessenda, L.C.R., 2009. Quaternary palaeoenvironments and relative sea-level changes in Marajó Island (Northern Brazil): Facies,  $\delta^{13}\text{C}$ ,  $\delta^{15}\text{N}$  and C/N. *Palaeogeogr. Palaeoclimatol. Palaeoecol.* 282 (1–4), 19–31. <https://doi.org/10.1016/j.palaeo.2009.08.004>.
- Meyers, Philip A., 1994. Preservation of elemental and isotopic source identification of sedimentary organic matter. *Chem. Geol.* 114 (3–4), 289–302. [https://doi.org/10.1016/0009-2541\(94\)90059-0](https://doi.org/10.1016/0009-2541(94)90059-0).
- Ogrinc, N., Fontolan, G., Faganeli, J., Covelli, S., 2005. Carbon and nitrogen isotope compositions of organic matter in coastal marine sediments (the Gulf of Trieste, N Adriatic Sea): indicators of sources and preservation. *Mar. Chem.* 95, 163–181. Doi: 10.1016/j.marchem.2004.09.003.
- Pereira, M.G., Anjos, L.H.C., Valladares, G.S., 2005. Organossolos: Ocorrência, gênese, classificação, alterações pelo uso agrícola e manejo. In: Vidal-Torrado, P., Alleoni, L. R.F., Cooper, M., Silva, A.P., Cardoso, E.J. (Eds.), *Tópicos em Ciência do Solo*, 4 ed. SBSC, Viçosa, pp. 233–276.
- Pessenda, L.C.R., Camargo, P.D., 1991. Datação radiocarbônica de amostras de interesse arqueológico e geológico por espectrometria de cintilação líquida de baixa radiação de fundo. *Quim. Nova* 14 (2), 98–105.
- Rossi, M., Queiroz Neto, J.P., 2011. Relação solo/paisagem em regiões tropicais úmidas: o exemplo da Serra do Mar em São Paulo, Brasil. *Revista do Departamento de Geografia* 14, 11–23. <https://doi.org/10.7154/RDG.2001.0014.0001>.
- Santos, R.D., Lemos, R.C., Santos, H.G., Ker, J.C., Anjos, L.H.C., Shimizu, S.H. 2015. Manual de descrição e coleta de solo no campo. 7ª ed. revisada e ampliada, Viçosa. Sociedade Brasileira de Ciência do Solo. p. 100.
- Santos, H.G., Jacomine, P.K.T., Anjos, L.H.C., Oliveira, V.A., Lumbrellas, J.F., Coelho, M. R., Almeida, J.A., Araujo Filho, J.C., Oliveira, J.B., Cunha, T.J.F., 2018. *Sistema Brasileiro De Classificação de Solos*. Embrapa, Brasília.
- Santos, O.A.Q., Silva Neto, E.C., Garcia, A.C., Fagundes, H.S., Diniz, Y.V.F.G., Ferreira, R., Pereira, M.G. 2020. Impact of land use on Histosols properties in urban agriculture ecosystems of Rio de Janeiro, Brazil. *Rev Bras Cienc Solo*. 44, e0200041. Doi: 10.36783/18069657rbc20200041.
- Schmidt, M.W.I., Torn, M.S., Abiven, S., Dittmar, T., Guggenberger, G., Janssens, I.A., Kleber, M., Kögel-Knabner, I., Lehmann, J., Manning, D.A.C., Nannipieri, P., Rasse, D.P., Weiner, S.S.E., Trumbore, 2011. Persistence of soil organic matter as an ecosystem property. *Nature* 478, 49–56. <https://doi.org/10.1038/nature10386>.
- Silva Neto, Eduardo Carvalho da, Pereira, Marcos Gervasio, Carvalho, Marcelo de Araujo, Calegari, Marcia Regina, Schiavo, Jolimar Antonio, de Paula Sá, Natália, dos Anjos, Lúcia Helena Cunha, Pessenda, Luiz Carlos Ruiz, 2019. Palaeoenvironmental records of Histosol pedogenesis in upland area, Espírito Santo State (SE, Brazil). *J. S. Am. Earth Sci.* 95, 102301. <https://doi.org/10.1016/j.jsames.2019.102301>.
- Silva Neto, Eduardo Carvalho da, Pereira, Marcos Gervasio, Anjos, Lúcia Helena Cunha dos, Calegari, Marcia Regina, Azevedo, Antônio Carlos, Schiavo, Jolimar Antonio, Pessenda, Luiz Carlos Ruiz, 2020. Phytoliths as paleopedological records of an histosol-cambisol-ferralsol sequence in Southeastern Brazil. *Catena* 193, 104642. <https://doi.org/10.1016/j.catena.2020.104642>.
- Soil Survey Staff, 2010. *Keys to soil taxonomy*, 11. ed. USDA-Natural Resources Conservation Service, Washington, p. 338.
- Soil survey staff, 2014. *Keys to soil taxonomy, Twelfth Edition*. Natural Resources Conservation Service, Washington, DC, USA.
- Stanek, W., Silc, T., 1977. Comparisons of four methods for determination of degree of peat humification (decomposition) with emphasis on the von Post Method. *Can. J. Soil Sci.* 57, 109–117. <https://doi.org/10.4141/cjss77-015>.
- Stuiver, M., Reimer, P.J., and Reimer, R.W. 2021. CALIB Radiocarbon Calibration C14 version 8.2. Access: <http://calib.org/calib/>. Accessed in: 2021-4-9.
- Teixeira, P.C., Donagemma, G.K., Fontana, A., Teixeira, W.G., 2017. *Manual de métodos de análise de solo*. Embrapa, Rio de Janeiro, p. 573p.
- Valladares, G.S., Pereira, M.G., Anjos, L.H.C., Benites, V.B., Ebeling, A.G., Mouta, R.O., 2007. Humic substance fractions and attributes of Histosols and related high-organic-matter soils from Brazil. *Commun. Soil Sci. Plan.* 38 (5–6), 763–777. <https://doi.org/10.1080/00103620701220759>.
- Vidal-Torrado, P., Ferreira, T.O., Otero, X.L., Souza-Jr, V.S., Ferreira, F.P., Andrade, G.R. P., Macías, F., 2010. Pedogenetic processes in mangrove soils. In: Otero, X.L., Macías, F. (Eds.), *Pedogenetic processes in mangrove soils*. Nova Science Publishers, New York, pp. 25–50.
- Zinck, J.A., 2011. Tropical and subtropical peats: an overview. In: *Peatlands of the Western Guayana Highlands, Venezuela*. Springer, Berlin, Heidelberg, pp. 5–28.